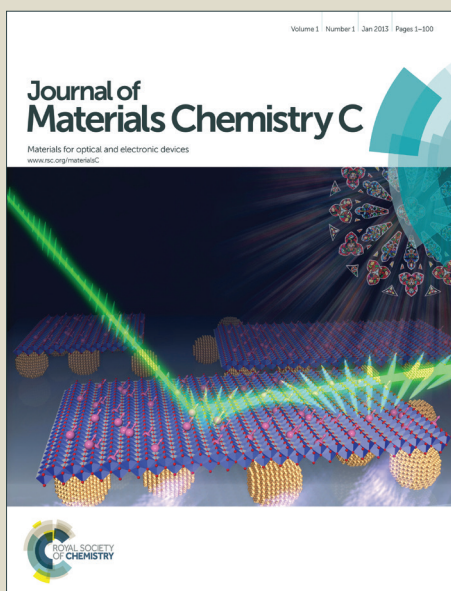


Journal of Materials Chemistry C

Accepted Manuscript



This is an *Accepted Manuscript*, which has been through the Royal Society of Chemistry peer review process and has been accepted for publication.

Accepted Manuscripts are published online shortly after acceptance, before technical editing, formatting and proof reading. Using this free service, authors can make their results available to the community, in citable form, before we publish the edited article. We will replace this *Accepted Manuscript* with the edited and formatted *Advance Article* as soon as it is available.

You can find more information about *Accepted Manuscripts* in the [Information for Authors](#).

Please note that technical editing may introduce minor changes to the text and/or graphics, which may alter content. The journal's standard [Terms & Conditions](#) and the [Ethical guidelines](#) still apply. In no event shall the Royal Society of Chemistry be held responsible for any errors or omissions in this *Accepted Manuscript* or any consequences arising from the use of any information it contains.

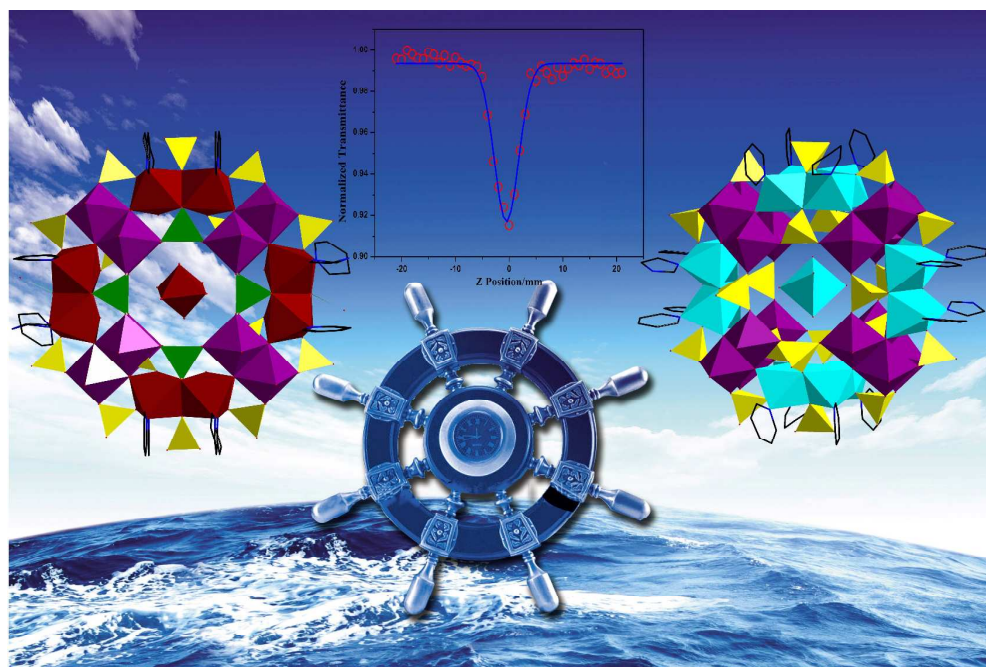
Cite this: DOI: 10.1039/c0xx00000x

www.rsc.org/xxxxxx

Two Novel Organic-Inorganic Hybrid Molybdenum(V) Cobalt/Nickel Phosphate Compounds Based on Isolated Nanosized Mo/Co(Ni)/P Cluster Wheels

Hao Miao,^a Hong-Xiang Wan,^a Ming Liu,^a Yu Zhang,^a Xiao Xu,^a Wei-Wei Ju,^a Dun-ru Zhu^a and Yan Xu^{*a, b}

5



10

Compounds **1** and **2** are the first two isolated structures in the family of 2D layered high-nuclear wheel-shaped {Mo/TM/P} clusters. Both compounds show good NLO activities that are rare in compounds containing POM anions.

15

Two Novel Organic-Inorganic Hybrid Molybdenum(V) Cobalt/Nickel Phosphate Compounds Based on Isolated Nanosized Mo/Co(Ni)/P Cluster Wheels

Hao Miao,^a Hongxiang Wan,^a Ming Liu,^a Yu Zhang,^a Xiao Xu,^a Weiwei Ju,^a Dunru Zhu^a and Yan Xu^{*a, b}

⁵ Received (in XXX, XXX) Xth XXXXXXXXXX 20XX, Accepted Xth XXXXXXXXXX 20XX

DOI: 10.1039/b000000x

Two high nuclear wheel-shaped nanoscale clusters,

[Co(H₂O)₆]₂{[C₃H₄N₂]₂[C₅NH₅]₁₄[H₁₅(Mo₂O₄)₈Co₁₆(PO₄)₁₄(HPO₃)₁₀(OH)₃]}·5H₂O (**1**) and

[C₃H₅N₂]₄[C₅NH₅]₂[Ni(H₂O)₆]₂{[C₃H₄N₂]₂[C₅NH₅]₁₄[H₁₈(Mo₂O₄)₈Ni₁₆(PO₄)₂₂(OH)₆]}·11H₂O (**2**), have

10 been successfully synthesized employing the Py and Imi ligands as chemical modifiers. The two clusters both take nanoscale wheel-like shapes, and the inorganic cores are wrapped up by the Py and Imi ligands acting as organic shells. In compounds **1** and **2**, the polyoxoanion unit exhibits a new organic-inorganic hybrid polymolybdophosphate, representing the first two isolated POMs in the wheel-type {Mo/TM/P} materials. While Py and Imi ligands improved electric delocalization effects of polyanions. It's worth 15 noting that the molecular TPA cross section σ of compound **1** is 2.5 times more than that of compound **2** which demonstrates that the nonlinear optical property can also be improved by replacing part of phosphate radicals with phosphite radicals through enhancing the electron delocalization.

Introduction

Polyoxometalates, one type of the well-known metal-oxo cluster 20 compounds that are attractive for their potential applications in catalysis, medical agents, electronic and magnetic materials.¹ The development of polyoxomolybdates depends on the synthesis of new materials possessing unique structures and rich properties.² One of the popular tactics is to design and synthesize the 25 molybdenum phosphates by incorporating transition metal phosphates with the polyoxomolybdates to form materials of multiproperty.³ In this respect, the reaction system of the molybdenum transition-metal phosphate {Mo/TM/P} under hydrothermal conditions is currently productive in isolation of 30 new polyoxomolybdates with novel structures and fulfilling properties.⁴ It is noteworthy that in this family most of the polyoxomolybdates are constructed by the following well-known building blocks, that is, the basket-like {Mo₁₈P₆} cage,⁵ Dawson-class {Mo₁₈P₂} cluster,⁶ the {Mo₁₆TM₁₆P₂₆} wheel,⁷ the Keggin-type {Mo_{12-x}TM_xP} unit,⁸ {Mo₆P₄} fragment⁹ and {Mo₅P₂} anion.¹⁰ In this study, one challenging work in this field is the construction of novel wheel-shaped {Mo₁₆TM₁₆P₂₆} polyoxometalates.¹¹ Furthermore, we pay particular attention to 40 wheel-shaped clusters not only because of their characteristic aesthetic architectures, also more importantly, their potential

application in nonlinear optical property as functional materials.

At present, the research on polyoxometalates in the field of nonlinear optics mainly focus on the classic Keggin and Dawson anions.^{12, 13} To the best of our knowledge, only six compounds 45 that contain wheel-shaped {Mo/TM/P} polymolybdophosphate clusters have been reported. In 2001, two 2D wheel-shaped molybdenum(v) cobalt phosphates based on [H₁₄(Mo₁₆O₃₂)Co₁₆(PO₄)₂₄(H₂O)₂₀]¹⁰⁻ were firstly reported by Francis Sécheresse et al.^{7a} Interestingly, they obtained the 50 analogous 2D compound with Ni(II) instead of Co(II), [H₁₈(Mo₂O₄)₈Ni₁₆(PO₄)₂₆(OH)₆(H₂O)₈]¹⁸⁻ in the following year.^{7b} Since then, another two new 2D wheel-shaped phosphomolybdates [H₃₀(Mo₁₆O₃₂)Ni₁₄(PO₄)₂₆O₂(OH)₄(H₂O)₈]¹²⁻ 11a and [H₁₈(Mo₁₆O₃₂)Co₁₆(H₂O)₁₈(PO₄)₂₄]⁶⁻ 11b have been 55 synthesized. In 2011, as continuing research work on wheel-type {Mo/TM/P} system, Yang's group applied organic ligands to decorate high-nuclear {Mo/TM/P} polymolybdophosphate clusters and made a new 2D layered molybdenum cobalt phosphate,

60 [H₂₄(Mo₁₆O₃₂)Co₁₆(PO₄)₂₄(OH)₄(C₁₀H₈N₂)₄(C₅H₄N)₂(H₂O)₆]⁴⁻ under hydrothermal conditions,^{11c} in which the organic ligands pyridine and 4,4'-bipyridine are introduced into the {Mo/TM/P} system, forming the first organic-inorganic hybrid polymolybdophosphate.

65 Above six reported wheel-type {Mo/TM/P} compounds are 2D layered structures, and adjacent wheel-type clusters are connected each other by covalent bonds. It is noteworthy that all the lacunary polyoxomolybdate compounds were synthesized by carefully controlling the reaction conditions.¹⁴ Presently, 70 literatures about polyoxometalates of functional complex materials mostly focus on magnetism, catalysis, electricity, but the reports on their nonlinear optical property are very rare, especially third-order optical properties. Since the shape and structure of wheel-type {Mo/TM/P} clusters are comparable 75 with fullerenes, it is therefore vital to design isolated wheel-type

^a College of Chemistry and Chemical Engineering, State Key Laboratory of Materials-oriented Chemical Engineering, Nanjing Tech University, Nanjing, 210009, P. R. China. Fax: (+) 86-25-83211563; E-mail: yanxu@njtech.edu.cn

^b State Key Laboratory of Coordination Chemistry, Nanjing University, Nanjing, 210093, P. R. China.

† Electronic Supplementary Information (ESI) available: Further experimental data and discussion. CCDC 992032 (**1**) and 992033 (**2**). For ESI and crystallographic data in CIF or other electronic format. See DOI: 10.1039/b000000x/

M-O clusters, in order to explore their third-order optical nonlinearities. However, we realized that the rigid ligand can also be employed as organic shells in the efficient construction of high-nuclear wheel-shaped {Mo/TM/P} clusters, since the rigid ligands have few or even no coordination modes and conformation changes when they are linked to the metal ions. If the monodentate ligands are used to decorate the surfaces of wheel-shaped clusters, terminal ligands will increase steric hindrance, prevent the connection between the wheels, and obtain isolated wheel structural materials.

In the present work, we have successfully synthesized two high nuclear wheel-shaped nanoscale clusters, $[\text{Co}(\text{H}_2\text{O})_6]\{[\text{C}_3\text{H}_4\text{N}_2]_2[\text{C}_5\text{NH}_5]_{14}[\text{H}_{15}(\text{Mo}_2\text{O}_4)_8\text{Co}_{16}(\text{PO}_4)_{14}(\text{HPO}_3)_{10}(\text{OH})_3]\}\cdot 5\text{H}_2\text{O}$ (**1**) and $[\text{C}_3\text{H}_5\text{N}_2]_4[\text{C}_5\text{NH}_5]_2[\text{Ni}(\text{H}_2\text{O})_6]\{[\text{C}_3\text{H}_4\text{N}_2]_2[\text{C}_5\text{NH}_5]_{14}[\text{H}_{18}(\text{Mo}_2\text{O}_4)_8\text{Ni}_{16}(\text{PO}_4)_{22}(\text{OH})_6]\}\cdot 11\text{H}_2\text{O}$ (**2**), employing the Py and Imi ligands as chemical modifiers. The two clusters both take nanoscale wheel-like shapes, and the inorganic cores are wrapped up by the Py and Imi ligands acting as organic shells. In compounds **1** and **2**, the polyoxoanion unit exhibits a new organic-inorganic hybrid polymolybdophosphate, representing the first two isolated POMs in the wheel-type {Mo/TM/P} materials. While Py and Imi ligands improved electric delocalization effects of polyanions. It's worth noting that the molecular TPA cross section σ of compound **1** is 2.5 times more than that of compound **2** which demonstrates that the nonlinear optical property can also be improved by replacing part of phosphate radicals with phosphite radicals through enhancing the electron delocalization.

Experimental

Synthesis of $[\text{Co}(\text{H}_2\text{O})_6]\{[\text{C}_3\text{H}_4\text{N}_2]_2[\text{C}_5\text{NH}_5]_{14}[\text{H}_{15}(\text{Mo}_2\text{O}_4)_8\text{Co}_{16}(\text{PO}_4)_{14}(\text{HPO}_3)_{10}(\text{OH})_3]\}\cdot 5\text{H}_2\text{O}$ (**1**)

A mixture of $\text{Co}(\text{OAC})_2\cdot 4\text{H}_2\text{O}$ (0.249 g, 1.001 mmol), $\text{H}_3\text{PMo}_{12}\text{O}_{40}\cdot 14\text{H}_2\text{O}$ (0.311 g, 0.150 mmol), imidazole (0.068 g, 1.001 mmol) and pyridine (5 ml) were dissolved in solution of 5 mL distilled water and 5 ml alcohol. The mixture was stirred for 1 h at room temperature. When the pH of the mixture was adjusted to about 6.0 with 50% H_3PO_3 , the suspension was put into a 25 mL Teflon-lined stainless-steel autoclave and kept under autogenous pressure at 150 °C for 3 days. After slow cooling to room temperature, red block crystals were filtered and washed with distilled water (40.18% yield based on Mo). Elemental analysis (%) calcd (found) for **1**: C 13.47(13.53), H 1.98(1.99), N 3.72(3.78). IR (solid KBr pellet, cm^{-1}): 3437 (s), 2974 (m), 1642 (s), 1378 (m), 1081 (m), 876 (w), 765 (w), 670(w), 567(w).

Crystal data for 1: $\text{C}_{76}\text{H}_{128}\text{N}_{18}\text{O}_{132}\text{P}_{24}\text{Co}_{17}\text{Mo}_{16}$, $M_r = 6686.09$, monoclinic crystal system, space group $C2/m$, $a = 29.724(4)$, $b = 24.623(3)$, $c = 20.687(3)$ Å, $\beta = 126.760(10)^\circ$, $V = 12130(2)$ Å³, $Z = 2$, $\rho_{\text{calcd}} = 1.845$ g cm⁻³, $\mu(\text{Mo}_{\text{K}\alpha}) = 2.172$ mm⁻¹, $1.23 \leq \theta \leq 25.02^\circ$, $R_{\text{int}} = 0.0621$, final $R_1 = 0.0696$ ($\omega R_2 = 0.2207$) for 10974 independent reflections [$I > 2\sigma(I)$]. Since some PO_4 , Py and Imi ligands are disordered, the relative P-O, C-N and C-C bond distances are restrained. The hydrogen atoms of organic ligands were refined in calculated positions, assigned isotropic thermal parameters, and allowed to ride on their parent atoms. While the H atoms for water molecules and HPO_3^{2-} ligands are not located.

Preparation of $[\text{C}_3\text{H}_5\text{N}_2]_4[\text{C}_5\text{NH}_5]_2[\text{Ni}(\text{H}_2\text{O})_6]\{[\text{C}_3\text{H}_4\text{N}_2]_2[\text{C}_5\text{NH}_5]_{14}[\text{H}_{18}(\text{Mo}_2\text{O}_4)_8\text{Ni}_{16}(\text{PO}_4)_{22}(\text{OH})_6]\}\cdot 11\text{H}_2\text{O}$ (**2**)

A mixture of $\text{Ni}(\text{OAC})_2\cdot 4\text{H}_2\text{O}$ (0.125 g, 0.501 mmol), $\text{H}_3\text{PMo}_{12}\text{O}_{40}\cdot 14\text{H}_2\text{O}$ (0.311 g, 0.150 mmol), imidazole (0.068 g, 1.001 mmol) and pyridine (5 ml) were dissolved in solution of 5 mL distilled water and 5 ml alcohol. The mixture was stirred for an hour at room temperature. When the pH of the mixture was adjusted to about 5.4 with 50% H_3PO_4 , the suspension was put into a 25 mL Teflon-lined stainless-steel autoclave and kept under autogenous pressure at 170 °C for 5 days. After slow cooling to room temperature, yellow block crystals were filtered and washed with distilled water (35.63% yield based on Mo). Elemental analysis (%) calcd (found) for **2**: C 16.24 (16.33), H 2.32 (2.39), N 5.41 (5.52). IR (solid KBr pellet, cm^{-1}): 3407 (s), 1630 (s), 1395 (s), 1084 (s), 970 (w), 760 (w), 557(w). **Crystal data for 2:** $\text{C}_{98}\text{H}_{166}\text{N}_{28}\text{O}_{143}\text{P}_{22}\text{Ni}_{17}\text{Mo}_{16}$, $M_r = 7238.97$, monoclinic crystal system, space group $P2_1/m$, $a = 20.603(18)$, $b = 21.832(19)$, $c = 25.821(2)$ Å, $\beta = 107.864(10)$, $V = 11055(17)$ Å³, $Z = 2$, $\rho_{\text{calcd}} = 2.172$ g cm⁻³, $\mu(\text{Mo}_{\text{K}\alpha}) = 2.553$ mm⁻¹, $1.40 \leq \theta \leq 25.50^\circ$, $R_{\text{int}} = 0.1188$, final $R_1 = 0.0615$ ($\omega R_2 = 0.1494$) for 20506 independent reflections [$I > 2\sigma(I)$]. Since some Py and Imi ligands are disordered, the relative C-N and C-C bond distances are restrained. The hydrogen atoms of organic ligands were refined in calculated positions, while the H atoms for water molecules are not located.

Results and discussion

Hydrothermal synthesis has recently been proved to be a powerful method in the synthesis of Pom-based organic-inorganic hybrid compounds. Many factors can affect the nucleation and crystal growth of final products during a specific hydrothermal synthesis, such as the type of initial reactants, starting concentrations of reactants, time, pH values, solvents and temperature. In our case, solvents (pyridine) play an important role for the formation of two isolated structures in the family of 2D layered high-nuclear wheel-shaped {Mo/TM/P} clusters. Pyridine not only acts as a solvent, but also serves on ligands link to the wheels, prevent the connection between the wheels, and obtain isolated wheel structural materials. In our parallel experiments, pyridine was replaced by water or alcohol in the synthesis, we only get powder impurities without crystals. It is also worth mentioning that all the reported 2D wheel-shaped {Mo/TM/P} clusters were made within the pH range of 2.0-4.0. Based on many experiments to obtain compounds **1** and **2** of isolated structures, we find the most suitable pH range is 5.0-6.0 in our synthetic method. In order to make clear the relationship of phosphorous acid and phosphoric acid in the synthesis of the two wheel-type clusters, the contrast experiment analyses were carried out. The results show that wheel-type Mo/Co/P cluster was obtained only by using phosphorous acid, while Mo/Ni/P cluster was synthesized only by phosphoric acid. In addition, the water instead of the mixture of alcohol and water be used as solvent for the experiments and just got some precipitation. Therefore the alcohol also plays an important role in the synthesis of compounds **1** and **2**.

Single-crystal X-ray diffraction analysis revealed that compound **1** is constructed from the isolated wheel-type cluster unit

$[H_{15}(Mo_2O_4)_8Co_{16}(PO_4)_{14}(HPO_3)_{10}(OH)_3]^{2-}$ (Figure 1) modified with Py and Imi ligands, $Co(H_2O)_6$ octahedron, and lattice water molecules (see Supporting Information Figure S1a). The structure building unit can be described as a centrosymmetric wheel-shaped cluster containing two types of four $\{Co_4P_6N_4\}$ units, four $\{Mo_4\}$ tetramers, encapsulating a central $[Co(H_2O)_6]^{2+}$ octahedron located on an inversion with overall C_{2v} symmetry (Figure 1). The outer size of the wheel-shaped cluster is $16.9 \times 16.9 \text{ \AA}$, while the inner cavity is $7.9 \times 8.1 \text{ \AA}$. Interestingly, PO_4 and HPO_3 are both existed in the cluster, while only one kind of PO_4 tetramer was encountered in the three reported $\{Mo_{16}Co_{16}P_{24}\}$ wheels.⁷ Except the $P(4)O_4$ and the $HP(6)O_3$ groups linked to four Co centers, all PO_4 and HPO_3 groups as bridges or hinges are joined to the $\{Co_4\}$ or $\{Mo_4\}$ tetramers to reinforce the wheel cluster and they can be separated into four types on the basis of the coordination environment of the PO_4 and HPO_3 groups, i.e., the two μ_4 - PO_4 groups and two μ_4 - HPO_3 groups bridge four Co atoms, the eight μ_4 - PO_4 groups bridge two Co and two Mo atoms, the four μ_5 - PO_4 groups bridge four Mo atoms and one Co atom and the eight μ_4 - HPO_3 groups bridge two Co and two Mo atoms.

In the wheel, two types of $\{Mo_4\}$ tetramers formed by the linkage of two $\{Mo_2(\mu-O)_2\}$ dimers containing four MoO_6 octahedra are reinforced by three phosphate groups (P1, P2, P10 for tetramer (Mo1Mo3) and P3, P5, P9 for tetramer (Mo2Mo4)) via a μ_3 -oxygen atom (O8 and O21, respectively) and six μ_2 -oxygen atom (O10, O11, O16 and O6, O7, O22, respectively) with Mo-Mo distances in the range of 2.602-2.607 \AA (see Supporting Information Figure S2a, b).

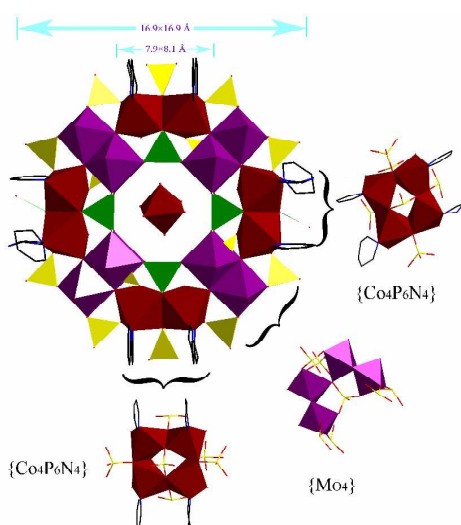


Fig. 1 Polyhedral representation of the hybrid wheel-shaped cluster of **1**. Color code: Co, dark red; Mo, violet; O, red; N, blue; C, black; HPO_3 , green; PO_4 , yellow.

Four $\{CoO_5N\}$ octahedra connect to each other in the edge-sharing manner and are further linked by PO_4 and HPO_3 groups in a corner-sharing manner to form two types of $\{Co_4\}$ tetramers. All the Co centers exhibit the six-coordination environment in an octahedral structure: In one type of $\{Co_4\}$ tetramer (see Supporting Information Figure S2c), the Co2 centers are coordinated with two μ_3 -O atoms shared by two Co atoms and two PO_4 groups, one μ_3 -O atom shared by two Co atoms and HPO_3 groups, one μ_3 -O atom shared by one Co atom and two Mo atoms,

one μ_2 -oxygen atom shared by two Co atoms and one N atom of one py ligand. The Co4 centers are surrounded by three μ_3 -O atoms shared by two Co atoms and PO_4 groups, one μ_3 -O atom shared by two Co atoms and HPO_3 groups, one μ_3 -O atom shared by one Co atom, two Mo atoms, and one N atom of one Py ligand. In the other type of $\{Co_4\}$ tetramer (see Supporting Information Figure S2d), the Co coordination environments are similar to the former except one Co5 center links to the N atom of the Imi ligand while other three Co centers link to the N atoms of the Py ligands. The μ_4 - $P(4)O_4$ group bridges four Co atoms is substituted by the μ_4 - $P(6)O_3$ group. The Co-O bond lengths are in the range of 2.033-2.292 \AA , and Co-N bond lengths are in the range of 2.100-2.143 \AA .

Interestingly, fourteen Py and two Imi groups as monodentate ligands make an organic shell to wrap the wheel-type cluster $[H_{15}(Mo_2O_4)_8Co_{16}(PO_4)_{14}(HPO_3)_{10}(OH)_3]^{2-}$ anion, and prevent the further connections between adjacent inorganic anions, while a novel isolated organic-inorganic hybrid wheel-type cluster anion, $\{[C_3H_4N_2]_2[C_5NH_5]_{14}[H_{15}(Mo_2O_4)_8Co_{16}(PO_4)_{14}(HPO_3)_{10}(OH)_3]^{2-}\}$ is generated. Furthermore, these isolated wheel clusters are further linked together via hydrogen-bonding to form a 3D supramolecular network. (Figure 2).

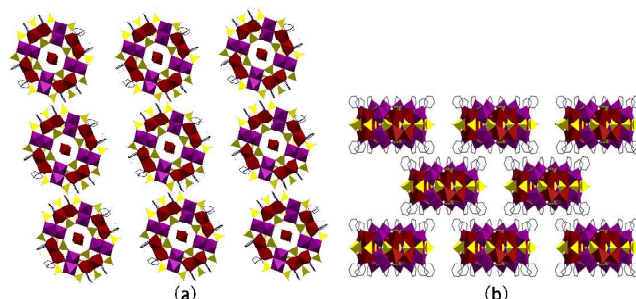


Fig. 2 (a) Polyhedral representation of the 3D framework of **1** along the b axis. (b) view of the 3D framework along the c axis. The H atoms and lattice water molecules are omitted for clarity.

Compared with **1**, compound **2** is constructed from the isolated wheel-type cluster unit $[H_{18}(Mo_2O_4)_8Ni_{16}(PO_4)_{22}(OH)_6]^{6-}$ (Figure 3) modified with Py and Imi ligands, $Ni(H_2O)_6$ octahedron, lattice water molecules, free Py and protonated Imi cations (see Supporting Information Figure S1b). Different to the two kinds of similar Co tetramers encountered in **1**, two kinds of Ni tetramers in **2** can be distinguished apparently, namely tetramer $\{Ni_4P_5N_4\}$ and $\{Ni_4P_6N_4\}$. As shown in Figure S3, the wheel-shaped cluster of **2** contains three kinds of building blocks, namely $\{Ni_4P_5N_4\}$ tetramer, $\{Ni_4P_6N_4\}$ tetramer and $\{Mo_4\}$ tetramer. Two $\{Ni_4P_5N_4\}$ tetramers and two $\{Ni_4P_6N_4\}$ tetramers are alternately connected by four $\{Mo_4\}$ tetramers in a corner-sharing manner to form the wheel with overall C_{2v} symmetry. The outer size of the wheel-shaped cluster is $20.1 \times 20.2 \text{ \AA}$, while the inner cavity is $9.2 \times 9.2 \text{ \AA}$ (larger than **1**).

All the Ni centers exhibit the six-coordination environment in a octahedral structure: In the $\{Ni_4P_5N_4\}$ tetramer (see Supporting Information Figure S3a), Ni1 and Ni2 connect with three O atoms derived from the three $\{PO_4\}$ groups, one N atom from the ligand (Imi for Ni1 and Py for Ni2), one μ_3 -O atom shared by two Mo centers and one Ni site and one μ_4 -O atom shared by four Ni centers. Ni5 and Ni8 connect with two O atoms derived from the two $\{PO_4\}$ groups, one N atom from the Py ligand, one μ_2 -O

atom shared by two Ni centers, one μ_3 -O atom shared by two Mo centers and one Ni site and one μ_4 -O atom shared by the four Ni centers. In the $\{\text{Ni}_4\text{P}_6\text{N}_4\}$ tetramer (see Supporting Information Figure S3b), the Ni6 and Ni7 centers are coordinated with four O atoms derived from the four $\{\text{PO}_4\}$ groups, one N atom from the Py ligand, one μ_3 -O atom shared by one Ni and two Mo centers. The Ni3 and Ni4 centers are coordinated with three O atoms derived from the three $\{\text{PO}_4\}$ groups, one N atom from the Py ligand, one μ_2 -O atom shared by two Ni centers and one μ_3 -O atom shared by one Ni and two Mo centers. On the basis of the above connection manners, four $\{\text{NiO}_5\text{N}\}$ octahedra are linked to each other in edge-sharing manner and further surrounded by $\{\text{PO}_4\}$ groups in corner-sharing manner. The Ni-O bond lengths are in the range of 2.005-2.294 Å, and Ni-N bond lengths are in the range of 2.017-2.108 Å.

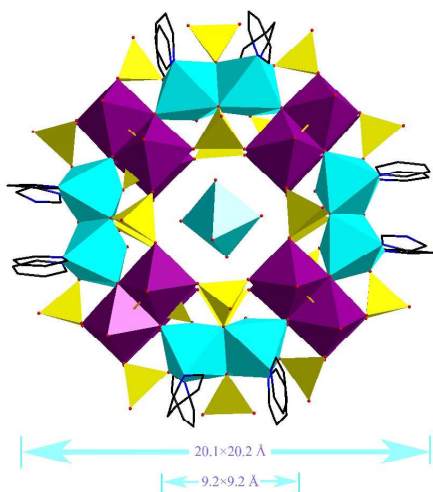


Fig. 3 Polyhedral representation of the hybrid wheel-shaped cluster of **2**.

The four $\{\text{Mo}_4\}$ tetramers can be regarded as two $\{\text{Mo}_2\text{O}_4\}$ fragments corner-linked into a V-type tetramer and surrounded by seven $\{\text{PO}_4\}$ groups, which is similar to the $\{\text{Mo}_4\}$ in **1** with the Mo-O bond lengths in the range of 1.668-2.433 Å (see Supporting Information Figure S3c).

It is noteworthy that the $\{\text{PO}_4\}$ groups in the wheel play an important role in linking and reinforcing the wheel-shaped polyoxoanion. Considering the coordination environment of $\{\text{PO}_4\}$ groups in the cluster, they can be separated into three types, that is the two μ_4 - PO_4 groups bridging four Ni atoms, the sixteen μ_4 - PO_4 groups bridging two Ni and two Mo atoms, the four μ_6 - PO_4 groups bridging four Mo atoms and two Ni atoms.

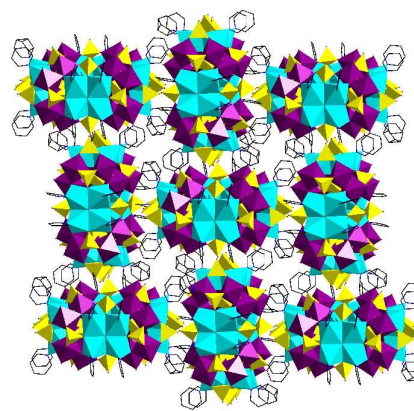


Fig. 4 Polyhedral representation of the 3D framework along the *b* axis in **2**. The H atoms, lattice water molecules, free Py and protonated Imi ligands are omitted for clarity.

Moreover, similar to **1**, **2** exhibits a new linking mode that in contrast to the reported 2D layered molybdenum(V) nickel phosphates as each wheel in **2** connects two Imi and fourteen Py ligands, forming a novel isolated organic-inorganic hybrid wheel-type cluster anion $\{[\text{C}_3\text{H}_4\text{N}_2]_2[\text{C}_5\text{NH}_5]_{14}[\text{H}_{18}(\text{Mo}_2\text{O}_4)_8\text{Ni}_{16}(\text{PO}_4)_{22}(\text{OH})_6]\}^{6-}$. Furthermore, the remaining $[\text{C}_3\text{H}_4\text{N}_2]^+$ cations and solvent molecules including Py and water are involved hydrogen-bonding interactions with wheel-type cluster anions to form a 3D supramolecular network (Figure 4). In the all six reported Mo/Co(Ni)/P cluster wheels, we can find that the wheel-shaped clusters are connected by $\{\text{CoO}_4\}/\{\text{NiO}_4\}$ or 4,4'-bipyridine linkers to form 2D structures. In our work, we employ Imi and Py linkers to modify the wheels and prevent the connection between the wheels and get the first two isolated POMs in the wheel-type $\{\text{Mo}/\text{TM}/\text{P}\}$ materials.

PXRD measurements for compounds **1-2** were determined at room temperature (see Supporting Information Figure S4 and S5), the diffraction peak positions of the experimental XRD patterns of **1** and **2** are in agreement with that of simulated XRD patterns, which indicate the phase purity of compounds **1** and **2**. The TG curve (Figure S6) of **1** shows a slight weight loss of 3.24% before 150 °C corresponds to the release of 11 coordinated and lattice water molecules (calc. 2.96%). The second weight loss of 19.68% from 150 to 600 °C is assigned to the removal of all imidazole and pyridine ligands and the dehydration of three hydroxyl groups (calc. 19.34%). The third weight loss of 8.25% in the temperature range of 600-690 °C might be attributed to the decomposition of partial P_2O_5 derived from the polyanion in compound **1**. The TG curve (Figure S7) of compound **2** is similar to that of compound **1**, also exhibits three weight loss steps. The first weight loss of 4.43% between 25 to 140 °C corresponds to the release of 17 coordinated and lattice water molecules (calc. 4.23%). The second weight loss of 23.78% between 140 to 440 °C is assigned to the removal of all imidazole and pyridine ligands and the dehydration of six hydroxyl groups (calc. 24.50%). The last weight loss of 8.47% in the temperature range of 440-750 °C might be attributed to the decomposition of partial P_2O_5 derived from the polyanion in compound **2**.

The luminescence studies of compounds **1-2** and the ligands imidazole and pyridine are explored in the solid state at room temperature. The emission bands are centered at about 406 nm

($\lambda_{\text{ex}} = 337 \text{ nm}$) for imidazole, and 427 nm ($\lambda_{\text{ex}} = 370 \text{ nm}$) for pyridine, which may attributed to the ligand-centered $\pi^*-\pi$ electronic transitions. Comparably, compounds **1** and **2** exhibit similar emission band at ca. 406 nm and 426 nm upon excitation at 255 nm (Figure S8 and S9). The emission intensity increases in comparison with free organic ligands, which may be owe to the hydrogen bonding interactions between the organic ligands and the guest water molecular effectively increase the rigidity of the ligands by reducing the loss of energy through thermal vibrations.

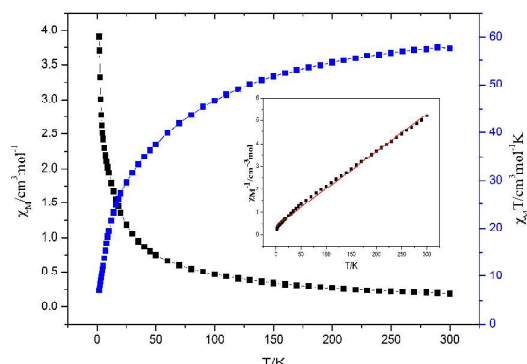


Fig. 5 Temperature dependence $\chi_M T$ (blue) and χ_M (black) (inset, χ_M^{-1}) for compound **1**.

The magnetic behavior of **1** has been investigated at 1000 Oe in the temperature $2\text{--}300 \text{ K}$ and are plotted in the form of χ_M versus T , $\chi_M T$ versus T and χ_M^{-1} versus T (inset) as shown in Figure 5. The wheel-shaped cluster contains four $\{\text{Co}_4\}$ connected with four $\{\text{Mo}_4\}$ in a corner-sharing manner besides the isolated $\text{Co}(\text{H}_2\text{O})_6$ cation in the center. Only the Co^{II} ions are responsible for the magnetic properties of **1** as the spin pairing of the d^1 electrons in the Mo^{V} dimers with the short Mo-Mo distances in an average value of 2.604 \AA .¹⁵ The $\chi_M T$ curve display a continuous decrease upon cooling from $57.58 \text{ cm}^3 \text{ mol}^{-1} \text{ K}$ at 300 K , which is a little higher than the calculated value of $51 \text{ cm}^3 \text{ mol}^{-1} \text{ K}$ for the 17 uncoupled Co^{II} ions ($S = 2$, $g = 2$), to $7.41 \text{ cm}^3 \text{ mol}^{-1} \text{ K}$ at 2 K , indicating significant antiferromagnetic exchange interactions in **1**. The χ_M^{-1} versus T plot can be fitted by the Curie-Weiss law with $C = 61.39 \text{ cm}^3 \text{ mol}^{-1} \text{ K}$ and $\theta = -24.21 \text{ K}$, respectively. The relative large and negative Weiss constants (θ) indicates the presence of mainly antiferromagnetic interaction and spin-orbit coupling effects.^{7a, 11c} Considering the M-O-M angle is the most important parameter in the magnetostructural correlation of the POM cores, the Co-O-Co bond angles range between 95.7° and 105.2° with an average angle of 99.4° are in the range anticipated for antiferromagnetic interactions¹⁶ and are consistent with the experimental observation.

The plots of χ_M versus T , $\chi_M T$ versus T and χ_M^{-1} versus T (inset) of **2** measured from 2 to 300 K in an applied magnetic field of 2000 Oe are shown in Figure 6. The $\chi_M T$ value for **2** at room temperature is $17.31 \text{ cm}^3 \text{ mol}^{-1} \text{ K}$, which is nearly the same as the expected value $17 \text{ cm}^3 \text{ mol}^{-1} \text{ K}$ for 17 uncoupled Ni^{II} ions ($S = 1$, $g = 2.0$). Upon cooling, the $\chi_M T$ value slowly decreases to $1.86 \text{ cm}^3 \text{ mol}^{-1} \text{ K}$ at 2 K , suggesting significant antiferromagnetic exchange interactions in **2**. The data fit to the Curie-Weiss law give the $C = 18.99 \text{ cm}^3 \text{ mol}^{-1} \text{ K}$ and $\theta = -28.79 \text{ K}$. The negative Weiss constants (θ) indicates the antiferromagnetic interaction between the Ni^{II} centers inside the $\{\text{Mo}_{16}\text{Ni}_{16}\text{P}_{22}\}$

core.^{7b, 11a}

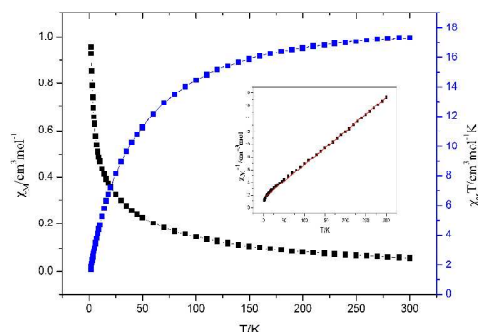


Fig. 6 Temperature dependence $\chi_M T$ (blue) and χ_M (black) (inset, χ_M^{-1}) for compound **2**.

The electronic spectrums of compounds **1** and **2** in water at a concentration of $1.0 \times 10^{-3} \text{ mol} \cdot \text{L}^{-1}$ give the liner absorption at room temperature. Two-photon absorption (TPA) values containing TPA coefficient β and TPA cross section σ were measured by the open-aperture Z-scan technique with femtosecond laser pulse and Ti:95 sapphire system (720 nm , 80 Hz , 140 fs).¹⁷ Figures 7 and 8 show the open aperture Z-scan curves of compounds **1** and $\mathbf{2}$ respectively. The unfilled circles are the experimental data and the solid line represents the theoretical simulated curve modified by the following equations:¹⁸

$$T(z, s = 1) = \sum_{m=0}^{\infty} \frac{[-q_0(z)]^m}{(m+1)^{3/2}} \quad \text{for } |q_0| < 1 \quad (1)$$

$$q_0(z) = \frac{\beta I_0 L_{\text{eff}}}{1 + z^2 / z_0^2} \quad (2)$$

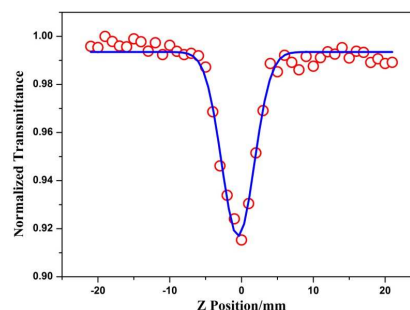


Fig. 7 The open aperture Z-scan data at 730 nm for compound **1** in water at $1.0 \times 10^{-3} \text{ mol L}^{-1}$. The unfilled circles are the experimental data and the solid curve represents the theoretical data.

where β is the TPA coefficient of the solution, I_0 is the input intensity of laser beam at the focus $z = 0$, $L_{\text{eff}} = (1 - e^{-\alpha L})/\alpha$ is the effective length with α and L are the linear absorption coefficient and the sample length respectively. z is the sample position, $z_0 = \pi \omega_0^2 / \lambda$ is the diffraction length of the beam, in which the ω_0 and λ are the spot size at the focus and the wavelength of the beam respectively. By using the equations mentioned above, we deduce the TPA absorption coefficient β are calculated as 0.01375 cm/GW and 0.0056 cm/GW for compounds **1** and **2**. Furthermore, the molecular TPA cross section σ can be calculated by the following relationship:

$$\sigma N_A d \times 10^{-3} = h\nu\beta \quad (3)$$

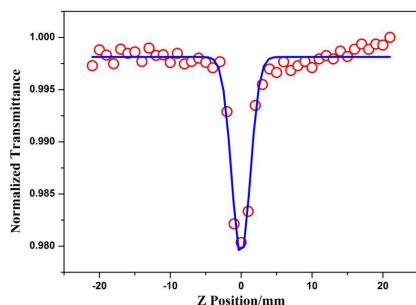


Fig. 8 The open aperture z-scan data at 750 nm for compound **2** in water at $1.0 \times 10^{-3} \text{ mol L}^{-1}$. The unfilled circles are the experimental data and the solid curve represents the theoretical data.

where N_A , d , h and ν are respectively the Avogadro's constant, the concentration of the compound, the Planck's constant and the frequency of input intensity. Based on Eq. (3), the molecular TPA cross section σ of compounds **1** and **2** were calculated as 622 GM and 247 GM (1 GM = $10^{-50} \text{ cm}^4/\text{s}/\text{photon}$), respectively. It was acknowledged that the extended π -electron delocalization in the structure resulted in the third-order NLO response. Up to now, the research on polyoxometalates in the field of nonlinear optics mainly focus on the classic Keggin and Dawson anions. The third-order NLO responses indicates that the wheel-shaped clusters compounds **1** and **2** have potential application in nonlinear optical field.¹⁹ To our knowledge, compound **1** has the biggest molecular TPA cross section σ in polyoxometalates.

Conclusions

In conclusion, two new organic-inorganic hybrid molybdenum(V) cobalt/nickel phosphate compounds based on isolated $[\text{H}_{15}(\text{Mo}_2\text{O}_4)_8\text{Co}_{16}(\text{PO}_4)_{14}(\text{HPO}_3)_{10}(\text{OH})_3]^{2-}$ and $[\text{H}_{18}(\text{Mo}_2\text{O}_4)_8\text{Ni}_{16}(\text{PO}_4)_{22}(\text{OH})_6]^{6-}$ wheel type polyanions with Py and Imi ligands as chemical modifiers have been successfully synthesized under hydrothermal conditions. Meaningfully, the wheel-shaped nanoscale clusters $\{\text{Mo}_{16}\text{Co}_{16}\text{P}_{24}\}$ and $\{\text{Mo}_{16}\text{Ni}_{16}\text{P}_{22}\}$ are modified by Py and Imi ligands via TM-N bonds to construct isolated structures. Compounds **1** and **2** are the first examples of isolated organic-inorganic hybrid wheel-type clusters in the $\{\text{Mo}/\text{TM}/\text{P}\}$ system and show improved nonlinear optics properties. Compound **1** shows very good NLO activities which are very rare in compounds containing POM anions. The successful synthesis of both compounds may open up possibilities for the design of new organic-inorganic hybrid POM-based materials by introducing various organic ligands.

Supplementary data

CCDC- 992032- and CCDC-992033 contain the supplementary crystallographic data for compound **1** and **2**. These data can be obtained free of charge via <http://www.ccdc.com.ac.uk/conts/retrieving.html>, or from Cambridge Crystallographic Data Centre, 12 Union Road, Cambridge CB2 1E2, UK; fax: (+44) 1223-336-033; or e-mail: deposit@ccdc.cam.ac.uk.

Acknowledgements

The authors acknowledge financial support from the National Natural Science Foundation of China (20971068/21171093) and Jiangsu province (BK2012823).

Notes and references

- (a) M. Sadakane, E. Steckhan, *Chem. Rev.*, 1998, **98**, 219; (b) M. T. Pope, A. Müller, *Angew. Chem.*, 1991, **103**, 56; *Angew. Chem. Int. Ed.*, 1991, **30**, 34; (c) X. L. Wang, C. Qin, E. B. Wang, Z. M. Su, Y. G. Li, L. Xu, *Angew. Chem.*, 2006, **118**, 7571; (d) Y. Xu, K. L. Zhang, Y. Zhang, X. Z. You, J. Q. Xu, *Chem. Commun.*, 2000, **2**, 153; (e) D. L. Long, E. Burkholder, L. Cronin, *Chem. Soc. Rev.*, 2007, **36**, 105.
- (a) H. Jin, Y. F. Qi, E. B. Wang, Y. G. Li, X. L. Wang, C. Qin, S. Chang, *Cryst. Growth Des.*, 2006, **6**, 2693; (b) P. Lightfoot, D. Masson, *Acta Crystallogr. Sect. C.*, 1996, **52**, 1077; (c) Y. Lu, J. Lü, E. B. Wang, Y. Q. Guo, X. X. Xu, L. Xu, *J. Mol. Struct.*, 2005, **740**, 159; (d) L. Xu, Y. Sun, E. Wang, E. Shen, Z. Liu, C. Hu, *J. Solid State Chem.*, 1999, **146**, 533.
- (a) P. Mialane, A. Dolbecq, L. Lisnard, A. Mallard, J. Marrot, F. Sécheresse, *Angew. Chem. Int. Ed.*, 2002, **13**, 2398; (b) Y. Z. Wang, H. L. Li, C. Wu, Y. Yang, L. Shi, L. X. Wu, *Angew. Chem. Int. Ed.*, 2013, **17**, 4577; (c) M. Tani, T. Sakamoto, S. Mita, S. Sakaguchi, Y. Ishii, *Angew. Chem. Int. Ed.*, 2005, **17**, 2586; (d) N. Kawasaki, H. Wang, R. Nakanishi, S. Hamanaka, R. Kitaura, H. Shinohara, T. Yokoyama, H. Yoshikawa, K. Awaga, *Angew. Chem. Int. Ed.*, 2011, **15**, 3471.
- (a) X. L. Wang, C. Qin, E. B. Wang, Z. M. Su, Y. G. Li, L. Xu, *Angew. Chem. Int. Ed.*, 2006, **44**, 7411; (b) A. Müller, S. K. Das, P. Kögerler, H. Bögge, M. Schmidtman, A. X. Trautwein, V. Schünemann, E. Krickemeyer, W. Preetz, *Angew. Chem. Int. Ed.*, 2006, **44**, 7411.
- (a) X. M. Zhang, H. S. Wu, F. Q. Zhang, A. Prikhod'ko, S. Kuwata, P. Comba, *Chem. Commun.*, 2004, **18**, 2046; (b) K. Yu, Y. G. Li, B. B. Zhou, Z. H. Su, Z. F. Zhao, Y. N. Zhang, *Eur. J. Inorg. Chem.*, 2007, **36**, 5662.
- (a) C. G. Liu, W. Guan, P. Song, Z. M. Su, C. Yao, E. B. Wang, *Inorg. Chem.*, 2009, **48**, 8115; (b) L. Xavier, B. Carles, P. Josep-M, S. Jose Pedro, *Inorg. Chem.*, 2003, **42**, 2634; (c) D. Lou, H. Q. Tan, W. L. Chen, Y. G. Li, E. B. Wang, *CrystEngComm.*, 2010, **12**, 2044.
- (a) C. du Peloux, A. Dolbecq, P. Mialane, J. Marrot, E. Rivière, F. Sécheresse, *Angew. Chem. Int. Ed.*, 2001, **40**, 2455; (b) C. du Peloux, A. Dolbecq, P. Mialane, J. Marrot, E. Rivière, F. Sécheresse, *Inorg. Chem.*, 2002, **41**, 7100.
- (a) Q. H. Zhang, C. J. Cao, T. Xu, M. Su, J. Zhang, Y. Wang, *Chem. Commun.*, 2009, **17**, 2376; (b) N. Kenji, Y. Kazunori, N. Yukihiro, K. Tada-aki, *J. Mol. Catal. A-Chem.*, 1997, **126**, 43; (c) A. X. Tian, J. Ying, J. Peng, J. Q. Sha, Z. M. Su, H. J. Pang, P. P. Zhang, Y. Chen, M. Zhu, Y. Shen, *Cryst. Growth Des.*, 2010, **10**, 1104.
- (a) L. A. Mundi, R. C. Haushalter, *Inorg. Chem.*, 1992, **31**, 3050; (b) L. A. Mundi, R. C. Haushalter, *Inorg. Chem.*, 1993, **32**, 1579; (c) J. P. Wang, J. W. Zhao, P. T. Ma, J. C. Ma, L. P. Yang, Y. Bai, M. X. Li, J. Y. Niu, *Chem. Commun.*, 2009, **17**, 2362.
- (a) Y. Ma, Y. Lu, E. B. Wang, X. X. Xu, Y. Q. Guo, X. L. Bai, L. Xu, *J. Mol. Struct.*, 2006, **784**, 18; (b) X. M. Lu, X. J. Wang, P. Z. Li, X. H. Pei, C. H. Ye, *J. Mol. Struct.*, 2008, **872**, 129; (c) Y. Lu, Y. G. Li, E. B. Wang, J. Lü, L. Xu, R. Clérac, *Eur. J. Inorg. Chem.*, 2005, **7**, 1239.
- (a) Y. N. Zhang, B. B. Zhou, Y. G. Li, Z. H. Su, Z. F. Zhao, *Dalton Trans.*, 2009, **43**, 9446; (b) Y. Ma, Y. G. Li, E. B. Wang, Y. Lu, X. Xu, X. L. Bai, *Transition Met. Chem.*, 2006, **31**, 262; (c) Y. Kai, B. B. Zhou, Y. Yu, Z. H. Su, G. Y. Yang, *Inorg. Chem.*, 2011, **50**, 1862.
- (a) Y. S. Zhou, J. Peng, E. B. Wang, L. J. Zhang, *Transition Met. Chem.*, 1998, **23**, 125; (b) L. Xu, E. B. Wang, Z. Li, D. G. Kurth, X. G. Du, H. Y. Zhang, C. Qin, *New J. Chem.*, 2002, **26**, 782; (c) J. Y. Niu, X. Z. You, C. Y. Duan, H. K. Fun, Z. Y. Zhou, *Inorg. Chem.*, 1996, **35**, 4211.
- (a) A. Muller, R. J. Cannon, A. N. Sarjeant, K. M. Ok, P. S. Halasyamani, A. J. Norquist, *Cryst. Growth Des.*, 2005, **5**, 1913; (b) X. M. Zhang, B. Z. Shan, C. Y. Duan, X. Z. You, *Chem. Commun.*, 1997, 1131. (c) H. Murakami, T. Kozeki, Y. Susuki, S. Ono, H. Ohtake, N. Sarukura, E. Ishikawa, T. Yamase, *Appl. Phys. Lett.*, 2001, **79**, 3564.

- 14 (a) X. L. Wang, C. Qin, E. B. Wang, Z. M. Su, *Chem.-Eur. J.*, 2006, **12**, 2680; (b) C. Streb, C. Ritchie, D. L. Long, P. Kögerler, L. Cronin, *Angew. Chem. Int. Ed.*, 2007, **46**, 7579; (c) J. M. Knaust, C. Inman, S. W. Keller, *Chem. Commun.*, 2004, **5**, 492; (d) Y. Q. Lan, S. L. Li, X. L. Wang, K. Z. Shao, Z. M. Su, E. B. Wang, *Inorg. Chem.*, 2008, **47**, 529.
- 5 15 P. J. Vergamini, H. Vahrenkamp, L. F. Dahl, *J. Am. Chem. Soc.*, 1971, **93**, 6327.
- 16 (a) K. Isele, F. Gigon, A. F. Williams, G. Bernardinelli, P. Franz, S. Decurtins, *Dalton Trans.*, 2007, **3**, 332; (b) Y. S. Xie, Q. L. Liu, H. Jiang, J. Ni, *Eur. J. Inorg. Chem.*, 2003, **22**, 4010.
- 10 17 (a) D. M. Li, Q. Zhang, P. Wang, J. Y. Wu, Y. H. Kan, Y. P. Tian, H. P. Zhou, J. X. Yang, X. T. Tao, M. H. Jiang, *Dalton Trans.*, 2011, **40**, 8170; (b) J. L. Hua, B. Li, F. S. Meng, F. Ding, S. X. Qian, H. Tian, *Polymer.*, 2004, **45**, 7143; (c) T. Geethakrishnan, P. K. Palanisamy, *Opt. Commun.*, 2007, **270**, 424.
- 15 18 (a) M. Sheik Bahae, A. A. Said, T. H. Wei, D. J. Hagan, E. W. Van Stryland, *IEEE J. Quantum Electron.*, 1990, **26**, 760; (b) W. Zhao, P. Paltty-Muhoray, *Appl. Phys. Lett.*, 1994, **65**, 673; (c) D. G. McLean, R. L. Sutherland, M. L. Brant, D. M. Brandelik, T. Pottenger, *Opt. Lett.*, 20 1993, **18**, 858.
- 19 (a) W. W. Ju, H. T. Zhang, X. Xu, Y. Zhang, Y. Xu, *Inorg. Chem.*, 2014, **53**, 3269; (b) Y. M. Xie, Q. S. Zhang, Z. G. Zhao, X. Y. Wu, S. C. Chen, C. Z. Lu, *Inorg. Chem.*, 2008, **47**, 8086; (c) T. R. Veltman, A. K. Stover, A. N. Sarjeant, K. M. Ok, P. S. Halasyamani, A. J. 25 Norquist, *Inorg. Chem.*, 2006, **45**, 5529.